

## EXPERIMENTS ON COLLISIONAL GRAIN CHARGING OF MICRON-SIZED PREPLANETARY DUST

TORSTEN POPPE, JÜRGEN BLUM, AND THOMAS HENNING

Astrophysical Institute and University Observatory, Schillergäßchen 3, 07745 Jena, Germany; poppe@astro.uni-jena.de

Received 1999 March 18; accepted 1999 November 15

### ABSTRACT

Collisions between micron-sized grains and larger objects with velocities up to several  $10 \text{ m s}^{-1}$  are believed to be an important physical process in the solar nebula with respect to the preplanetary dust aggregation. Former collision experiments demonstrated that grain-target collisions of micron-sized particles were marked by obvious electrostatic effects. Among those were the observation of particles which, after mechanical rebound, returned to the target and finally stuck, and of particle deposition on targets influenced by the presence of conducting materials. Therefore, it is clear that the dust aggregation process cannot adequately be described without investigating collisional grain charging experimentally. We present experiments on the collisional grain charging of micron-sized grains impacting target surfaces which, in contrast to former work, consist both of nonconducting material and the experiments involving smaller particles than before. Collisional grain charging is stronger than previously discussed with respect to preplanetary grains and should be considered concerning the preplanetary dust aggregation, the formation of lightning in the solar nebula, and a coupling of charged grains to magnetic fields.

*Subject headings:* accretion, accretion disks — dust, extinction — methods: laboratory — solar system: formation

### 1. INTRODUCTION

The planet formation process is believed to have started with a dust aggregation phase in the dilute gas of the accretion disk around the young Sun (Beckwith, Henning, & Nakagawa 1999). In order to investigate the dust aggregation process, we performed analogous experiments on single grain collisions with monodisperse silica spheres and with irregularly shaped diamond, enstatite, and silicon carbide grains (Poppe, Blum, & Henning 2000, hereafter Paper I). During experiments with all types of particles, trajectories of particles accelerated toward the target were observed. Many of the images showed rebounded particles returning to the target, which literally jumped on the surface. In a few cases, even successive jumps were imaged, indicating that the particles would finally stick, although the capture velocity was exceeded during the first collision. The obvious explanation is the action of electrostatic forces that must therefore be regarded as important for the dust aggregation. Knowledge of collisional charging helps to improve our understanding of the collisional mechanics observed in the former experiments that were presented in Paper I. From the astrophysical point of view, collisional grain charging is not only important for the efficiency of the dust aggregation process. It also has influences on other physical conditions in the early solar nebula because (1) charged particles can interact with magnetic fields and (2) collisional particle charging and subsequent charge separation can cause electrical discharges in the dilute gas of the early nebula. Electrical discharge heating has long been discussed to be a possible cause for the chondrule formation in the early solar nebula (e.g., Horányi & Robertson 1996; Love, Keil, & Scott 1995; Gibbard, Levy, & Morfill 1997 and references therein).

#### 1.1. Previous Work Important for Collisional Grain Charging

Contact and frictional electrification has been known longer than any other cause of electricity. Nevertheless, tribocharging is poorly understood. “No model” describes

“the phenomenon satisfactorily” (Vercoulen 1995) and there is “no firmly established theory of contact electrification” (Lowell 1986a). Reproducible experimental results on contact electrification are difficult to obtain because the electrification of surfaces is very sensitive to numerous conditions that are hard to identify or to control in experiments and that make contact and frictional electrification “temperamental to the extend of reversing sign without obvious reason” (Harper 1967). Among the influential parameters are the surface material, the contact pressure, the way of surface cleaning, the orientation of crystalline structure, the roughness, the temperature, the size of the object to which the surface belongs, and the rubbing or gliding velocity between the surfaces.

Often, the attempt is made to distinguish between contact charging and frictional charging. Contact charging was introduced because charging also occurs if no rubbing is involved, as it is known from the contact of liquid mercury with insulating materials. Former work was intended to lead to a triboelectric series of materials that can be used to predict the sign of charging for contact among any two materials. However, these series are not free of contradictions (Vercoulen 1995). Frictional charging is responsible if two identical objects are charged by rubbing (Harper 1967). Note that often (e.g., Harper 1967) an important distinction is made between rubbing (with high-pressure contact belonging to frictional electrification) and gliding (with low-pressure contact belonging to contact electrification although motion is involved). However, almost always both types of charging occur in a surface contact and, moreover, the two types of electrification cannot easily be associated with a certain type of charge transfer. Types of charge transfer discussed are the migration of electrons or ions following an electrical field, the migration of electrons or ions against an electrical field due to diffusion, and the transfer of chemical or particulate impurities or of rubbed-off bulk material, all of which could carry charges (Harper 1967).

The former work reflects rather confusing knowledge on contact and frictional charging, and often the work is restricted to order-of-magnitude considerations or mea-

surements (Harper 1967; Lowell 1986a; Lowell 1986b). Nevertheless, there are important earlier results to bear in mind when working with collisional grain charging. (1) Apart from chemical effects of specially coated materials (Horn, Smith, & Grabbe 1993), the maximum surface charge density does not exceed  $10^{-4} \text{ C m}^{-2}$ , corresponding to 625 elementary charges per  $\mu\text{m}^2$ . Harper (1967) mentioned 20 electrostatic units of charge ( $= 6.66 \times 10^{-5} \text{ C m}^{-2}$ ) as maximum surface charge density, and Lowell (1986a) calls  $10^{-4} \text{ C m}^{-2}$  the limit and experimentally finds in vacuum  $5.4 \times 10^{-5} \text{ C m}^{-2}$ . Effects that are possibly responsible for this limit are discharge through air, spreading of surface charges from locally and temporarily higher charged surface spots until the charge density is reached that can permanently be carried, or electrical field built up by the charging process that acts against further charging (Harper 1967). (2) There is no fundamental difference in the charging between two insulating and between one insulating and one metallic surface in nongliding or nonrubbing contact. Lowell (1986a) points out that metals fitted into triboelectric series, suggesting that the charge transfer is of the same nature as among insulators. He experimentally verifies that the contact charging in vacuum between these two cases can differ by a small factor, but not by an order of magnitude. (3) A precharge carried on a surface is not shared with an uncharged or oppositely charged surface upon short contacts between insulators. Lowell (1986b) did not find that a precharged needle-like instrument tipping on a surface in vacuum shared its precharge. Based on this, one can predict that there should be no important electrical conductivity in a bouncing collision between insulating grains.

Charge transfer in particle collisions is important for terrestrial thunderstorms. Lacking other detailed studies, many authors applied such results on astrophysical problems or discussed the relevance for astrophysical applications (Morfill, Spruit, & Levy 1993; Gibbard et al. 1997, 1999; Love et al. 1995). The role of liquid water or rimming wet ice is important for many mechanisms of charge transfer, thus restricting their relevance in our context. Apart from the role of liquid water, other important problems with work on thunderstorm lightning are that the size of preplanetary grains is generally believed to be much smaller than the size of terrestrial hail or graupel and that the role of the surrounding air in thunderstorms must be considered. With respect to our experiments with  $\text{SiO}_2$  grains impacting  $\text{SiO}_2$  targets, an interesting aspect of ice-grain charging in thunderstorms is that the size of the objects decides about the sign of charge that is preferably acquired, since the precipitation of large, mainly positively charged ice grains results in building up the electrical field of thunderstorms, although both small and large grains consist of ice. In contrast to charging effects influenced by liquid water, the Elster-Geitel effect is an inductive charging process in a preexisting electrical field. The colliding objects obtain a conductive contact and the preexisting electrical field causes a charge transfer. Then the objects are separated such that the preexisting electric field is strengthened and the charging of further colliding objects will thus exponentially increase with time. In the past, the Elster-Geitel effect was partially regarded as a possibly important charging mechanism (Pilipp, Hartquist, & Morfill 1992; Morfill et al. 1993) and partially refused as such (Gibbard et al. 1997; Pilipp et al. 1998) because the charge transfer is extremely

weak. The Elster-Geitel effect requires a conductive contact which, for short-duration contacts of nonconductive materials, limits its effectiveness. Without understanding the detailed physics of grain charging and without data on the charge-transfer efficiency of colliding stony particles, one has the poor choice between either applying the results found for ice in thunderstorms on stony material in the solar nebula as done by Love et al. (1995) or restricting the work to the icy grains in the solar nebula as done by Gibbard et al. (1997). Therefore, Love et al. (1995) pointed out the need for laboratory measurements of the charge transfer for grains consisting of chondrule precursor material. The results on grain charging in thunderstorms (Illingworth 1985; Keith & Saunders 1994; Norville, Baker, & Latham 1991) on which today's assumptions on grain charging in the solar nebula are based predicts a weak charging compared to all charging strengths reported later in this paper. According to Gibbard et al. (1997), an ice sphere of  $1.2 \mu\text{m}$  diameter would acquire one elementary charge upon a bouncing collision with  $10 \text{ m s}^{-1}$  impact velocity.

In Paper I, we presented considerations for the choice of analogous materials and stated that the collisional behavior of nonconducting materials is mainly, though not exclusively, of importance. However, the experimental database on collisional grain charging known to the authors is restricted to collisions between grains and targets of which the target always consisted of an electrically conducting material. One reason for the choice of conducting targets may be that the collisional charge determination was often based on measuring the charge flowing away from the impacted surface. For example, John (1995) and John, Reisch, & Devour (1980) presented and discussed work which was motivated by an instrument called the "contact charge monitor," which measured the particle flux in aerosols by determining the collisional contact charge created on a metallic probe inside the instrument. John et al. (1980) determined the collisional contact charge transferred by NaCl and methylene blue particles depending on precharge and impact velocity. Charge transfer is found to be a function of precharge and sensitive to surface material and surface cleaning. A linear dependence of charge transfer from impact velocities between 30 and  $150 \text{ m s}^{-1}$  for  $2.5\text{--}4 \mu\text{m}$  diameter methylene blue particles impacting on stainless steel was measured. Some more work is reported on the charge transfer of millimeter-sized insulating objects impacting metal targets (Yamamoto & Scarlett 1986; Vercoolen 1995, and references therein). However, there are no experiments on the charge transfer of submicron particles (John 1995), the charge transfer in collisions between micron-sized particles and surfaces both consisting of insulating material must be investigated, and experimental data on the charge transfer among grains made of astrophysically relevant stony material are missing.

## 2. EXPERIMENTAL

### 2.1. Collisional Charging Strength of Silica Spheres

Silica spheres of  $0.5$  and  $1.2 \mu\text{m}$  diameter and the targets made of polished silica and a silicon wafer as described in Paper I were also used for the grain charging experiments. The setup of the dust grain collision experiment described in Paper I and in Poppe et al. (1997) was modified in order to measure the electric charge of the particles. A dust jet of

single grains is formed in vacuum by pushing a dust powder onto the front side of a fast rotating cogwheel. Coming in touch with the cogwheel, the dust sample is deagglomerated and accelerated upward, leading to a dust jet of single grains that impact a target with a wide velocity range up to several  $10 \text{ m s}^{-1}$ . Only  $10\text{--}40 \text{ }\mu\text{m}$  away from the target, the particle trajectories are optically imaged. The trajectory imaging system, which was previously used only to determine flight direction and velocity, in principal also allows measurement of the acceleration of the particles. Thus, for the highly monodispersed silica spheres of  $0.5$  and  $1.2 \text{ }\mu\text{m}$  diameter, the charge of the particles can be determined if an electrical field of known strength is applied. The electrical field was created parallel to the impact surface by two flat electrodes with a distance of  $2$  or  $3 \text{ mm}$  and a potential difference of  $10 \text{ kV}$ . Figure 1 (*left*) shows the arrangement for the polished silica target and (*right*) the alternative setup for the smooth silicon wafer. Both targets are described in more detail in Paper I.

The electrodes were designed such that they extended far to the bottom, which ensures that the approaching particles travel a distance of  $20 \text{ mm}$  for the silica target, or  $16 \text{ mm}$  for the silicon wafer, through the electrical field before impacting the target. This means that the trajectories of pre-charged particles approaching the target are inclined, allowing extraction of highly precharged particles before they reach the target and allowing determination of the charge of the particles approaching the target by observing the inclination of the trajectory. Thus, we could determine not only the charge of the particle rebounding, but the net collisional charging, i.e., how many elementary charges the particles acquire during the collisions in addition to their precharge. Typically, the precharge of the particles that could pass the electrical field of the capacitor plates was found to be smaller by 1 order of magnitude than the charge acquired in the subsequent collision. This means that the  $0.5 \text{ }\mu\text{m}$  diameter particles generally, but not always, were uncharged prior to impact. Figure 2 presents two typical

examples of trajectories to investigate collisional grain charging. The left image shows a bouncing particle that is attracted by the left (positive) electrode leading to a curved trajectory. The right image shows a collision in which the collisional charging and the energy loss upon collision is sufficient to attract the particle by the charged target such that it returns and finally sticks.

For the determination of the particle charge, the local electric field acting on the particle must be known. Due to the comparable size of electrode width and distance, due to the location of the silica target at the edge of the capacitor, and due to the presence of the targets close to the observed volume, the electric field strength is weakened compared to a field in a plate capacitor of infinite size. The weakening of the electrical field can be determined by fitting the charge measurements of the  $0.5 \text{ }\mu\text{m}$  diameter spheres to a scale of integer numbers as necessary for elementary charges. By doing that, we found that the electrical field directly beneath the quartz target is by a factor of  $2.4$  weaker than that of an ideal plate capacitor, and the one directly beneath the silicon wafer target is reduced by a factor of  $1.4$ .

Figure 3 shows the number of acquired elementary charges as a function of impact velocity for each pair of grain and target. The accuracy of the charge measurement primarily depends on the accuracy of the acceleration measurement. The narrow mass distribution of the highly monodispersed particles is of minor importance. As the precision of the acceleration measurement is increasing for longer particle trajectories and for slower particle velocities, individual errors of the charge determination vary heavily. Here, the error bars exclusively represent the dominating error due to the acceleration measurement. An error due to uncertainties in the determination of the electric field applied does not affect the data points relative to each other. The number of separated elementary charge varies strongly between individual collision. The typical number of charges acquired upon collision increases with increasing impact velocity. It is roughly 1 order of magnitude higher

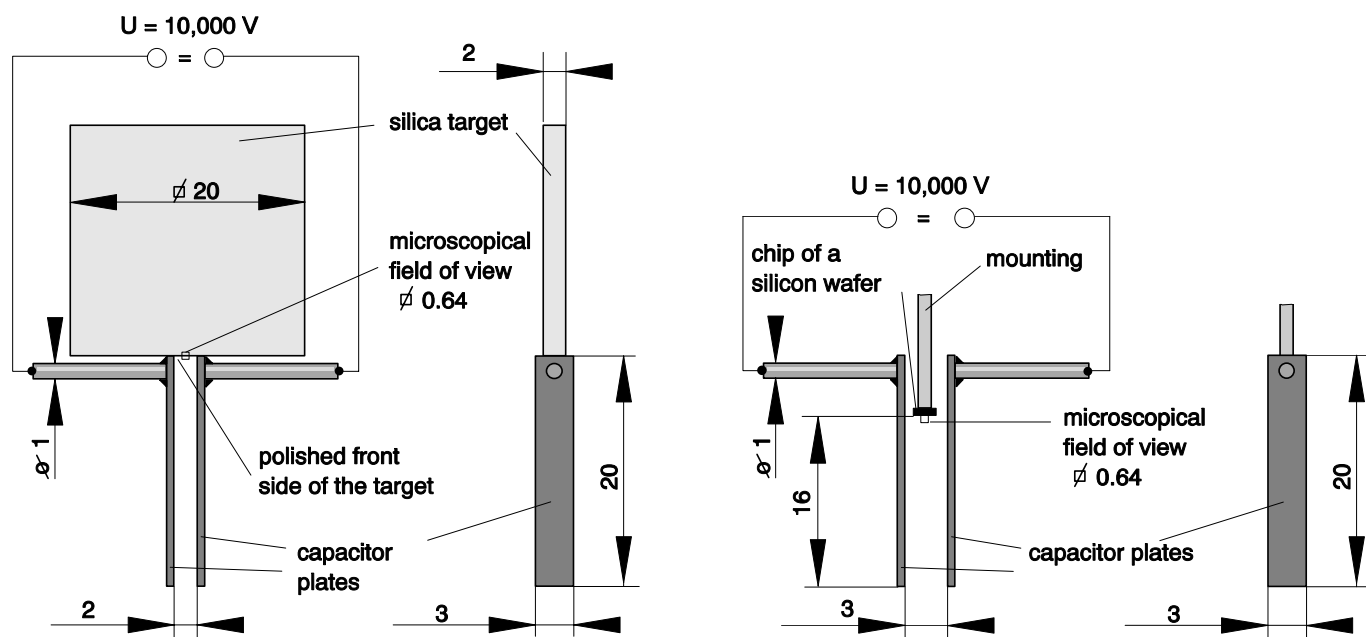


FIG. 1.—Geometrical arrangement for the collisional charging experiments with the polished silica target (*left*) and with the silicon wafer (*right*). The particles approach from the bottom.

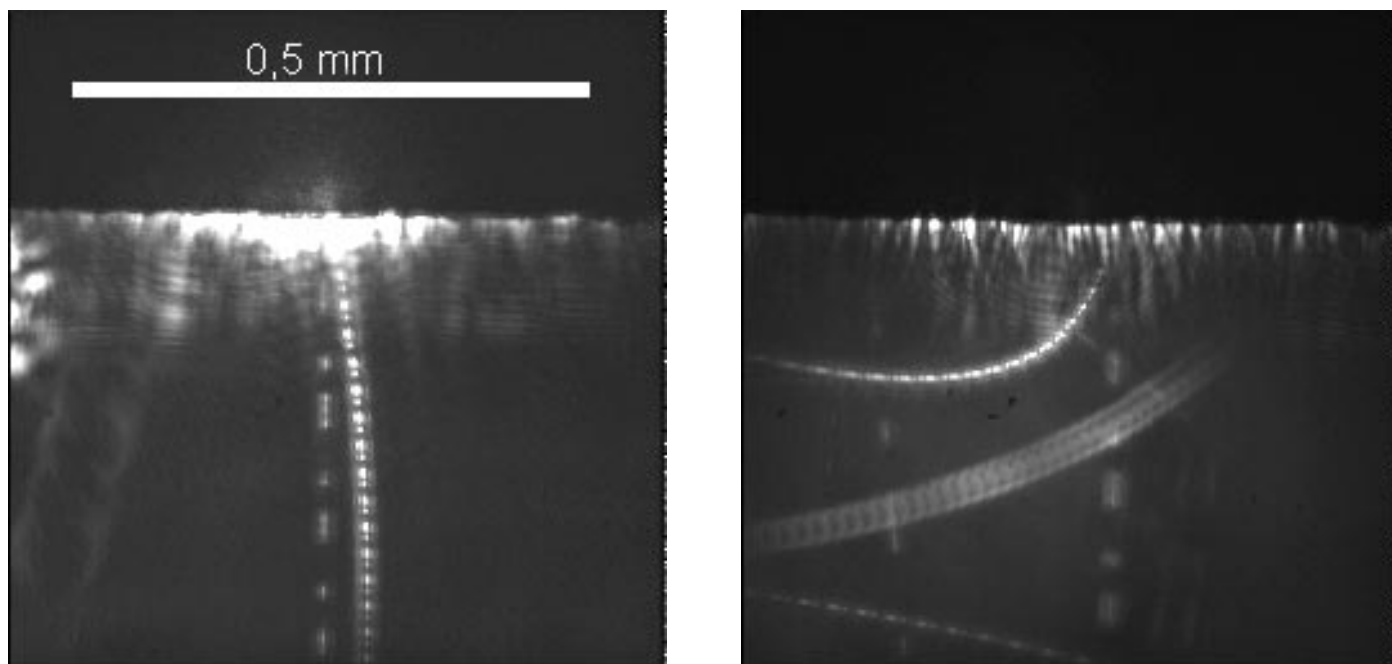


FIG. 2.—Uncharged silica spheres of  $0.5\ \mu\text{m}$  diameter impacting a polished silica target. The particle on the left bounces off and the accelerated (i.e., *curved*) rebound trajectory can be used to determine the charge acquired upon collision. The particle on the right undergoes sufficient energy loss and collisional charging upon impact to be attracted by the target after rebound. This shows that collisional charging can finally cause sticking, although a mechanical rebound occurs during the first contact.

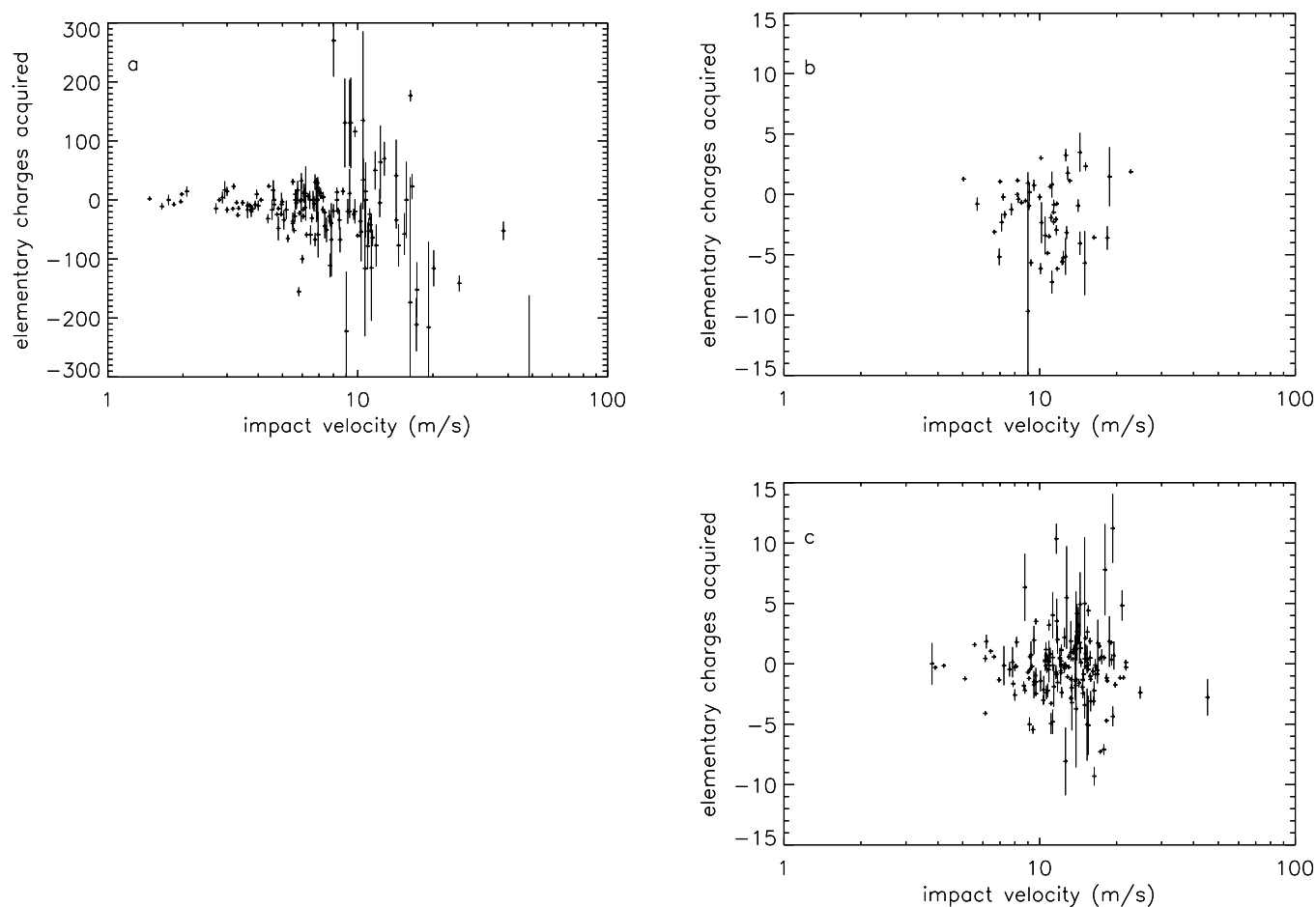


FIG. 3.—Collisional charging as a function of impact velocity for silica spheres of  $1.2\ \mu\text{m}$  impacting polished silica (*left*), of  $0.5\ \mu\text{m}$  diameter impacting polished silica (*right*), and of  $0.5\ \mu\text{m}$  spheres impacting the silicon wafer (*bottom*). Note the different vertical scales for the two types of incident particles.

for the 1.2  $\mu\text{m}$  diameter silica spheres than for the 0.5  $\mu\text{m}$  spheres, which is quite similar to the mass ratio of the two particle sizes. Eighty-four percent of charge separations in collisions between silica spheres and the silica target resulted in negatively charged particles and a positively charged target. With the silicon wafer and the 0.5  $\mu\text{m}$  diameter silica spheres, the number of positive and negative charges was quite in equilibrium, i.e., 48% of the elementary charges acquired were negative.

A better representation of collisional grain charging is obtained if we create a diagram of the number of separated elementary charges versus impact energy for collisions between both types of grains and both types of targets (Fig. 4). It makes it obvious that our measurements describe a collisional charging process whose absolute value of charge transfer  $|Q|$  is roughly proportional to the collisional energy  $E_{\text{kin}}$ . Assuming a power law, the best fit is obtained with

$$|Q| = \left( \frac{E_{\text{kin}}}{10^{-15} \text{ J}} \right)^{0.83}. \quad (1)$$

The number of elementary charges acquired for a certain impact velocity varies over 1 order of magnitude. The average number of separated elementary charges per unit impact energy falls between  $10^{14} \text{ J}^{-1}$  and  $10^{15} \text{ J}^{-1}$  in the impact energy range between  $10^{-15} \text{ J}$  and  $10^{-12} \text{ J}$ .

The charge density in the contact area between two spherical particles must be at least of the order of  $10^{-4} \text{ C m}^{-2}$ . This minimum charge density would require that a 1.2  $\mu\text{m}$  diameter sphere that gets charged with 300 elementary charges obtains a contact area of  $0.5 \mu\text{m}^2$ . Although the real contact area is unknown and cannot be estimated by the assumption of purely elastic deformation since our former work with these particles showed that (1) an effective energy dissipation upon impact takes place, which suggests plastic deformation and (2) the particles, in general, rotate, which suggests rolling or sliding (Paper I), such a large contact zone is unlikely. This means that the charge density in the contact area is by a small factor, but not by orders of magnitude, larger than  $10^{-4} \text{ C m}^{-2}$ , which is the maximum

equilibrium charge density reported in literature (see § 1.1). Since the contact area increases with increasing impact velocity and the rotational state differs from collision to collision, a charge transfer proportional to the contact surface is a possible explanation to account for both the increasing absolute value of the charge transfer with increasing collisional energy and the strong variation of charge transfer in individual collisions.

In Poppe & Blum (1997) and Paper I we discussed the possibility that high collisional charging causes the strong energy losses upon bouncing collisions with impact velocities of only a few  $\text{m s}^{-1}$ . However, we found that charging with several hundred elementary charges occurs only for velocities in excess of a few  $10 \text{ m s}^{-1}$ , so that we can now also exclude this possibility. This means that the loss of kinetic energy (as presented in Paper I) has no electrostatic but mechanical reasons.

## 2.2. Surface Charge Density

Charged particles were horizontally accelerated in the electrical field created by the high-voltage capacitor, according to Figure 1. Additionally, the particles were vertically accelerated by the electrical field caused by the surface charge on the target. Examples for images suitable for determining the relation between horizontal and vertical fields are shown in Figure 5. The vertical field has almost exactly half the field strength of the horizontal field. The charge density on the surface  $Q/A$  can be calculated by

$$\frac{Q}{A} = E_v \epsilon_0, \quad (2)$$

where  $E_v$  is the vertical field strength and  $\epsilon_0$  is the dielectric constant of vacuum. Thus, we found that the best value for the charge density on the polished surface of the silica target was  $9.2 \times 10^{-6} \text{ C m}^{-2}$ . Since the particles are charged in the collisions, it is plausible to assume that the target charging stems from this process too. This means that further collisions should increase the charge density on the target. However, we never found a charge density on the target that significantly differed from the above-mentioned value. This indicates that the target rapidly acquires a saturation charge density. According to § 1.1, such a limit to the charge density could be caused by electrical discharge, e.g., through air, local spreading of charges on temporarily higher charged spots, or by an electrical field built up due to former charging and acting against further charging. However, further charging of silica grains takes place indicating that the saturation charge density is not caused by impediments of the collisional charging process such as inhibiting further charge transfer due to an electric field caused by former charge transfer. Considering the dust-jet density and the typical number of charge separations in a single collision, we conclude that the charge density in the contact area, which according to § 2.1 is  $\geq 10^{-4} \text{ C m}^{-2}$ , is reduced by a local spreading of charges rather than by a discharge. The initial charge density is reduced to a saturation value of  $\approx 10^{-5} \text{ C m}^{-2}$ , which can permanently be carried by the surface and which is not reduced by a further spreading or discharge. The existence of the saturation charge density of  $\approx 10^{-5} \text{ C m}^{-2}$  on silica caused by local charge spreading is also supported by the maximum charge of the 1.2  $\mu\text{m}$  diameter spheres. This charge density corresponds to 288 elementary charges and, according to Figure

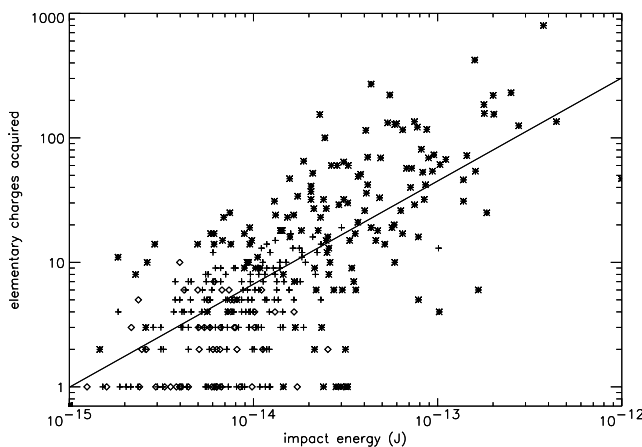


FIG. 4.—Absolute value of elementary charges acquired upon impact for both types of particles and targets as a function of impact energy. An asterisk indicates a 1.2  $\mu\text{m}$  diameter particle impacting polished quartz, a diamond represents a 0.5  $\mu\text{m}$  diameter particle impacting polished quartz, and a cross denotes a 0.5  $\mu\text{m}$  diameter particle impacting the silicon wafer. Most collisions had velocities between 10 and  $20 \text{ m s}^{-1}$ . The slope of the line corresponds is 0.83.

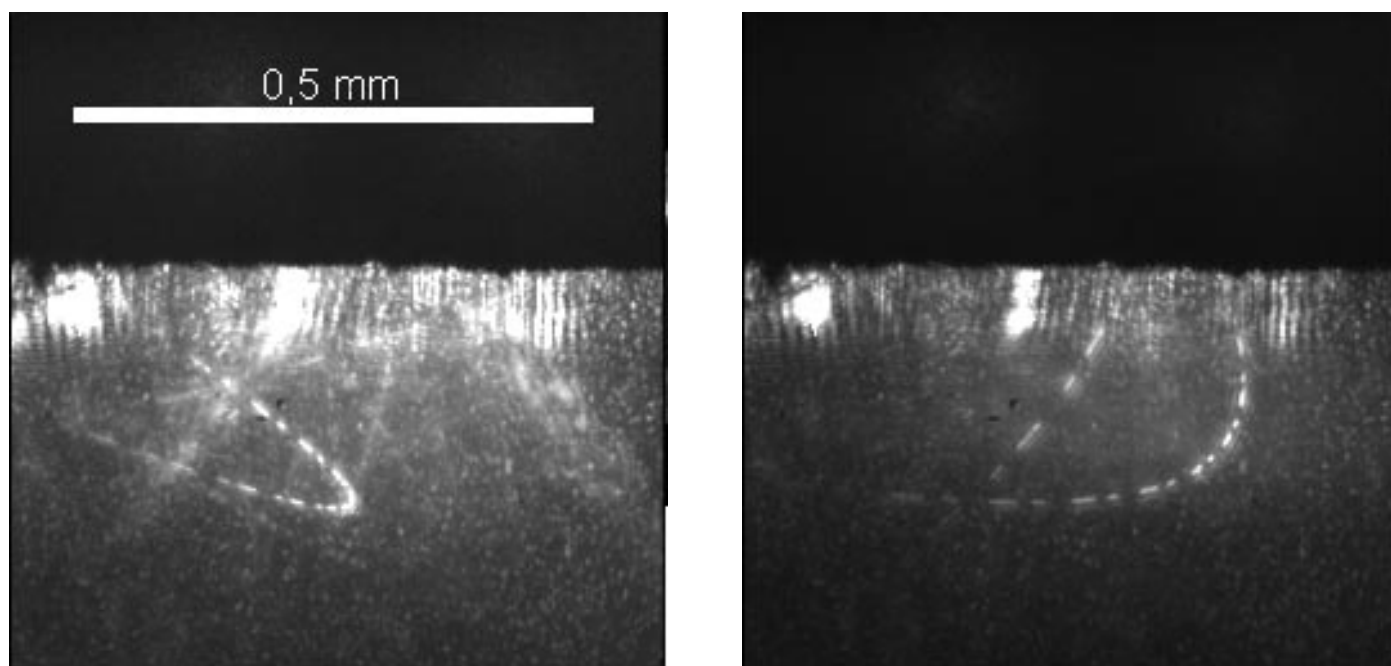


FIG. 5.—*Left*: Jumping silica sphere of  $1.2\ \mu\text{m}$  diameter leaves the target at the upper left and is both decelerated in the horizontal field of the capacitor and attracted to the top in the vertical field originating in the target. Such images can be used to determine the vertical field strength and, thus, the charge density on the target. *Right*: Image of an  $1.2\ \mu\text{m}$  diameter silica sphere approaching the target from the lower left (thereby being decelerated by the horizontal field) and impacting the polished quartz target. The rebound is faster than the impact, but the electrical charge has not changed sufficiently to explain the translational energy gain. Hence, other explanations for the translational energy gain must be considered.

4, these particles, in general, do not acquire more than 300 elementary charges.

### 2.3. Properties of “Jumping Particles”

Particles jumping over the target due to electrostatic effects occurred with all types of particles described and used in Paper I. However, these events were particularly abundant for the diamond grains with an average diameter of  $1.5\ \mu\text{m}$  and for the silica spheres of  $1.2\ \mu\text{m}$  diameter. Concerning the latter, we can, with the knowledge of the charge density on the silica target and of the charging strength, point out typical properties of jumping particles. Many of our recorded images show jumping particles as in Figure 2 (*right*) and Figure 5. Four images show two successive jumps, and one image—on which Figure 6 is based—shows three jumps. These successive jumps show impact velocities around  $2\ \text{m s}^{-1}$ , acceleration levels toward the target between  $5000$  and  $12,000\ \text{m s}^{-2}$ , and jump heights of several  $100\ \mu\text{m}$ . No change of acceleration in successive jumps was found, indicating that the particles neither significantly gained further charge nor lost precharge. Assuming 200 elementary charges on a  $1.2\ \mu\text{m}$  diameter  $\text{SiO}_2$  sphere,  $200\ \mu\text{m}$  jump height, and  $2\ \text{m s}^{-1}$  impact velocity at target contact, an acceleration of  $10,000\ \text{m s}^{-2}$  is necessary, which is well in the observed range. A vertical electrical field causing such an acceleration needs as its source, according to equation (2), a charge density of  $5 \times 10^{-6}\ \text{C m}^{-2}$ . This is half the value discussed in § 2.2, which shows that the assumed values have the correct order of magnitude and fit together reasonably well. The assumed particle charge may be explained by a single charging event with no further charging or discharging. According to § 2.1, a collisional charging with 200 elementary charges can be attributed to an impact velocity between  $15$  and  $47\ \text{m s}^{-1}$ . Such an initial impact velocity is plausible considering the

dust-jet generation, which is described in Poppe et al. (1997) and Paper I.

### 2.4. No Evidence for Collisional Discharge or Sharing of Precharge

It was never found that a particle lost charge upon impact or that a sharing of precharge occurred. Rather, even the trajectories of highly charged particles as shown in Figure 5 (*right*) and Figure 6 showed that no recombination of positive charge from the target and negative charge from the particle occurred upon contact. One could regard a positive grain charging as a type of charge shared with the positively precharged target. However, the observed charging strength rules out this possibility. According to § 2.3, the permanent charge density on the target is at least 1 order of magnitude lower than the charge transfer density at the area of contact. This means charge sharing would lead to a weaker charging and, thus, the collisional charging would be 1 order of magnitude less if it were positive compared to negative charging. Figure 4 shows that this is not the case, and this means that the collisional charge separation is no sharing of precharge. This also means that the electrical conductivity upon collisional contact is not important.

In Paper I, a few collisions were presented that were marked by a gain of translational energy upon impact, i.e., that the particles bounced off faster than they had approached. One of several possible explanations to account for this observation was that the particles hit a highly charged spot, shared the charge accumulated on that spot, and were accelerated by the repulsive electrostatic forces. The lack of any evidence for charge sharing is the reason why, as already mentioned in Paper I, we do not believe that electrostatic effects cause the gain of translational kinetic energy. Rather, the cause must be found in the mechanics that are discussed in Paper I. Additionally,

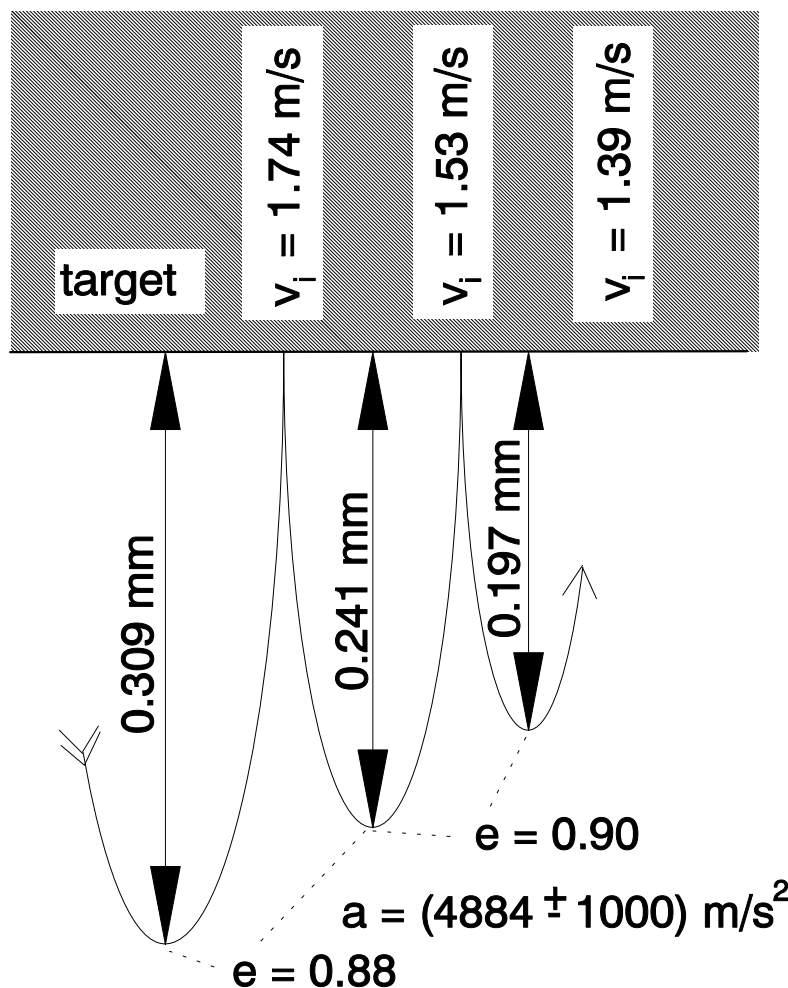


FIG. 6.—Particles attracted by the target can perform successive “jumps” with decreasing heights until they finally stick to the target. The solid line shows the trajectory of a  $1.2\ \mu\text{m}$  diameter silica sphere of which three successive jumps on the silica target were imaged. In this case, no voltage was applied to the horizontal capacitor. Jump heights, acceleration level  $a$ , and coefficients of restitution  $e$  (rebound velocity divided by impact velocity) are shown.

the experimental setup that was modified for the contact charge experiment allows us to present one counterexample of a particle that gained translational energy, although no change of its electrical charge was found. Figure 5 (right) shows a  $1.2\ \mu\text{m}$  diameter silica sphere which, after being reflected from the target, again impacted the silica target with  $215 \pm 4$  elementary charges and subsequently left it with  $213 \pm 34$  elementary charges (based on the mass of an ideal diameter of  $1.2\ \mu\text{m}$ ). The charge state before and after impact makes it extremely likely that the approaching and rebounded trajectories do belong to the same particle. The vertical component of impact velocity was  $2.5\ \text{m s}^{-1}$  and the rebound velocity  $4.9\ \text{m s}^{-1}$ , and both were determined about  $130\ \mu\text{m}$  away from the point of collision.

### 2.5. Electrostatic Influence on Dust Deposition of Diamond Grains

For adjustment purposes, some of the plate-shaped quartz targets have a grid of conducting material printed on the front and back side with the polished impact surface perpendicular in between as shown in Figure 7 (left). These targets were not used for the experiments on collisional grain charging with the arrangement shown in Figure 1 (left) in order to prevent the electrical field of the electrodes

being influenced by the conducting imprints. However, quartz targets with these imprints were used for the collision experiments without applied electrical field presented in Paper I.

Compared to all other types of particles discussed in Paper I, the diamonds of  $1.5\ \mu\text{m}$  average diameter showed a special behavior dramatically indicating the importance of electrostatic effects for the dust aggregation. The targets were exposed to a uniform dust flux, but were unevenly covered by a dust layer after the experimental runs. No particles were deposited in the close vicinity of the conducting imprint, whereas a few  $100\ \mu\text{m}$  away toward the target center there was an even and dense layer of single particles as shown in Figure 7 (right). On the same target, the dust layer toward the outer ends outside the range of the imprints was even, not only in the center, but also toward the edges. This means that, in this case, particle sticking exclusively occurred with electrostatic effects involved. The particles were highly charged upon impact and were reflected off the target, but then were attracted back to the target by its electric field. Close to the imprints the electric field (caused by the surface charge on the quartz target) was partially compensated by mobile electrons in the conducting imprint. This effect leads exclusively to a final deposi-

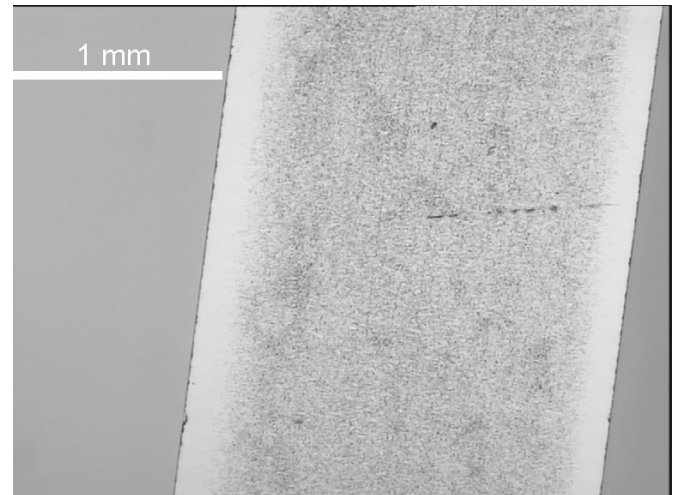
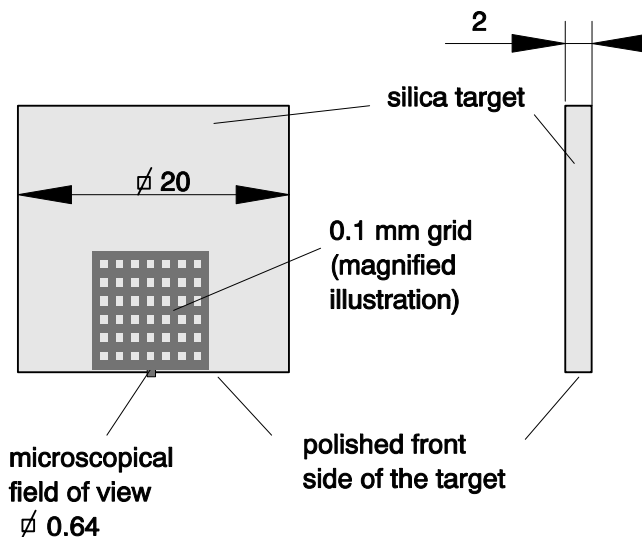


FIG. 7.—*Left*: Target with conducting imprint on the sides perpendicular to the polished impact surface as used for collision experiments without applied electrical field in Paper I. *Right*: Diamond grains of  $1.5\ \mu\text{m}$  mean diameter are deposited on the polished surface of the quartz target only some  $100\ \mu\text{m}$  away from the edges where the conducting imprint (not visible here) prevents the formation of an even dust layer.

tion some  $100\ \mu\text{m}$  away from conducting parts. We conclude that nonconducting materials collect dust better than metallic targets.

### 3. SUMMARY AND DISCUSSION

We measured the collisional grain charging of micron- and submicron-sized silica spheres impacting polished silica and atomically smooth (oxidized) silicon. To our knowledge, these are the first measurements of collisional charging with submicron-sized grains and the first measurements with micron-sized grains between two insulating materials. Furthermore, the grain charging was determined for silica, which is regarded as an abundant material of the solar nebula (Gail 1998) and represents properties of the important material class of silicates (Pollack et al. 1994). According to Weidenschilling & Cuzzi (1993), micron-sized objects collide with decimeter-to meter-sized objects embedded in the nebular gas with velocities of a few  $10\ \text{m s}^{-1}$  in 1 AU solar distance. The sizes of targets and particles and the collisional velocities cover these astrophysically relevant ranges.

We found that a  $1.2\ \mu\text{m}$  diameter silica sphere can acquire up to a few hundred elementary charges upon a bouncing collision with some  $10\ \text{m s}^{-1}$ . The transfer charge density at the point of contact is at least of the order of  $10^{-4}\ \text{C m}^{-2}$ . This temporarily and locally high-charge density is reduced by a local charge spreading to a charge density of  $10^{-5}\ \text{C m}^{-2}$ , which can permanently be carried by silica particles and by the silica target. The charge transfer efficiency varies strongly between individual collisions, but its mean value is roughly proportional to the collisional energy. A possible explanation is that the number of separated elementary charges is proportional to the contact area and that both the charge transfer density at the surfaces in contact and the permanent charge density limits the grain charging. Collisional grain charging was observed with all types of grains (silica, diamond, enstatite, silicon carbide) and both target materials (silica, silicon wafer) and should, therefore, be regarded as typical for preplanetary dust collisions. However, it is especially important for

grains of one micron diameter or slightly larger, as we have found in the experiments that electrostatic effects played an outstanding role for the  $1.5\ \mu\text{m}$  diamond grains and the  $1.2\ \mu\text{m}$  diameter silica spheres. Much larger grains having a smaller surface-to-mass ratio are limited by the maximum surface charge density of  $\approx 10^{-5}\ \text{C m}^{-2}$  and their increasing masses make them relatively unaffected by electrostatic forces. On the other hand, smaller grains possess both too small contact areas upon collision and too small collisional energies that do not lead to sufficient grain charging. The charge that a particle acquires is mostly negative, although both target and particle consist of silica and have the same temperature. Possibly, simply the size relation of the objects plays a role for the sign of charge as it is the case with ice grains in terrestrial thunderstorms.

The charge density and the charge transfer density are within known charge densities reported previously for insulating materials (see § 1.1). Nevertheless, the collisional charging is by 1–2 orders stronger than previously assumed in numerical simulations involving collisional grain charging in the solar nebula (Love et al. 1995; Gibbard et al. 1997). It is in agreement with work by Lowell (1986b) that no charge sharing was found among insulating materials, and that conductivity of surface charge was not important in a collision. Because of this and because of the observed strength of collisional charging, we conclude that the Elster-Geitel effect should no longer be considered for collisional grain charging of insulating grains in the solar nebula.

Collisional grain charging can directly contribute to the efficiency of the preplanetary dust aggregation because grains that mechanically rebounded can subsequently be trapped by collision-induced electrostatic fields. Not only the strong charge transfer efficiency, but also the substantial energy dissipation upon bouncing collisions (Paper I) contribute to the efficiency of this process. In the frame of the model of Weidenschilling & Cuzzi (1993), micron-sized grains and bodies of decimeter to meter size collide with several  $10\ \text{m s}^{-1}$  due to interactions with the dilute gas at 1 AU solar distance. Although the capture thresholds described in Paper I are exceeded by these velocities, colli-



sions can finally lead to sticking and, hence, to an efficient electrostatic agglomeration of the small particles on the runaway bodies.

Collisional dust grain electrification in the early solar nebula has long been discussed to be a cause for lightning, which could explain the melting of meteoritic chondrule precursors. Although this explanation is, compared to others, not favored today (Boss 1996), it is still seriously under discussion (Horányi & Robertson 1996); the strong grain charging found in our experiments supports this idea and may also direct attention to stony chondrule precursors, not just to icy grains as done previously (Gibbard et al. 1997).

Presently, the motion of particles in the solar nebula is believed to be exclusively caused by gravitation and aerodynamical gas forces (Weidenschilling & Cuzzi 1993). However, charged particles are also influenced by magnetic fields. The action of magnetic forces on particles could influence the spatial dust distribution in the solar nebula and the relative velocities in collisions. Moreover, in cases in which magnetic forces cause fast enough collisions, further collisional charging could lead to a self-sustained collisional grain charging process. So far, the strength and direction of magnetic fields in accretion disks are rather unknown, which makes it difficult to decide whether magnetic forces are possibly dominating over aerodynamical forces. However, although there is no direct observational evidence for magnetic fields in stellar accretion disks at small scales, the observation of winds and outflows is explained by magnetocentrifugal acceleration mechanisms that require the existence of a magnetic field with a strength of  $\approx 10^{-4}$  T at 1 AU solar distance (Königl & Ruden 1993). The field

strength mentioned is also supported by meteoritic evidence (Levy & Sonett 1978). Therefore, the field strength of  $\approx 10^{-4}$  T could be called “representative” (Königl 1997). The experiments showed that a grain of mass  $m = 10^{-15}$  kg can acquire  $n = 100$  elementary charges upon a collision with a few  $10 \text{ m s}^{-1}$ . The magnetic force on such a charged grain is then

$$F_{\text{mag}} = nq|\mathbf{v} \times \mathbf{B}|, \quad (3)$$

where  $\mathbf{v}_{pb}$  is the relative velocity between the magnetic field and the particle and  $q$  is the elementary charge. If we assume that magnetic forces are important if  $F_{\text{mag}}$  exceeds the aerodynamical headwind force the particle undergoes when spiraling inward, which is calculated according to Weidenschilling & Cuzzi (1993) in the order of  $10^{-20}$  N at 1 AU, we find that  $|\mathbf{v}_{pb}| \approx 10 \text{ m s}^{-1}$  may be sufficient to influence the particle motion. If the solar nebula was (partially) weakly ionized, ambipolar diffusion can occur, which means that the magnetic field that is frozen into the ions drifts relative to the neutral gas. In this case,  $\mathbf{v}_{pb}$  can reach several percent of the Keplerian velocity (Li 1996), which leads to a magnetic force exceeding the aerodynamical forces on the particle chosen as an example. These considerations show that magnetic forces on micron-sized particles in the solar nebula will be worth further investigation.

We thank the Alfried Krupp von Bohlen und Halbach-Stiftung, the Deutsches Zentrum für Luft und Raumfahrt (D. L. R.), and the Deutsche Forschungsgemeinschaft (D. F. G.) for funding of the present work.

#### REFERENCES

- Beckwith, S. V. W., Henning, T., & Nakagawa, Y. 1999, in *Protostars and Planets IV*, ed. V. Mannings, A. Boss, & S. Russell (Tucson: Univ. Arizona Press), in press
- Boss, A. P. 1996, in *Chondrules and the Protoplanetary Disk*, ed. R. H. Hewins, R. H. Jones, & E. R. D. Scott (Cambridge: Cambridge Univ. Press), 257
- Gail, H.-P. 1998, *A&A*, 322, 1099
- Gibbard, S. G., Levy, E. H., Lunine, J. I., & de Pater, I. 1999, *Icarus*, 139, 227
- Gibbard, S. G., Levy, E. H., & Morfill, G. E. 1997, *Icarus*, 130, 517
- Harper, W. R. 1967, *Contact and Frictional Electrification* (Oxford: Clarendon)
- Horányi, M., & Robertson, S. 1996, in *Chondrules and the Protoplanetary Disk*, ed. R. H. Hewins, R. H. Jones, & E. R. D. Scott (Cambridge: Cambridge Univ. Press), 303
- Horn, R. G., Smith, D. T., & Grabbe, A. 1993, *Nature*, 366, 442
- Illingworth, A. J. 1985, *J. Geophys. Res.*, 90, 6026
- John, W. 1995, *Aerosol Sci. & Technol.*, 23, 1
- John, W., Reisch, G., & Devor, W. 1980, *J. Aerosol Sci.*, 11, 115
- Keith, W. D., & Saunders, C. P. R. 1994, *J. Geophys. Res.*, 94, 13013
- Königl, A. 1997, in *IAU Coll. 163, Accretion Phenomena and Related Outflows*, ed. D. T. Wickramasinghe, L. Ferrario, & G. V. Bicknell (ASP Conf. Ser. 121; San Francisco: ASP), 551
- Königl, A., & Ruden, P. 1993, in *Protostars and Planets III*, ed. E. Levy & J. Lunine (Tucson: Univ. Arizona Press), 641
- Levy, E. H., & Sonett, C. P. 1978, in *Protostars and Planets*, ed. T. Gehrels (Tucson: Univ. Arizona Press), 516
- Li, Z.-J. 1996, *ApJ*, 465, 855
- Love, S. G., Keil, K., & Scott, E. R. D. 1995, *Icarus*, 115, 97
- Lowell, J. 1986a, *J. Phys. D*, 19, 95
- . 1986b, *J. Phys. D*, 19, 105
- Morfill, G., Spruit, H., & Levy, E. H. 1993, in *Protostars and Planets III*, ed. E. Levy & J. Lunine (Tucson: Univ. Arizona Press), 939
- Norville, K., Baker, M., & Latham, J. 1991, *J. Geophys. Res.*, 96, 7463
- Pilipp, W., Hartquist, T. W., & Morfill, G. E. 1992, *ApJ*, 387, 364
- Pilipp, W., Hartquist, T. W., Morfill, G. E., & Levy, E. H. 1998, *A&A*, 331, 121
- Pollack, J. B., et al. 1994, *ApJ*, 421, 1595
- Poppe, T., & Blum, J. 1997, *Adv. Space Res.*, 20(8), 1595
- Poppe, T., Blum, J., & Henning, T. 1997, *Rev. Sci. Instrum.*, 68(6), 2529
- . 2000, *ApJ*, 533, 454 (Paper I)
- Vercoulen, P. 1995, Ph.D. dissertation, Delft Tech. Univ.
- Weidenschilling, S. J., & Cuzzi, J. N. 1993, *Formation of Planetesimals in the Solar Nebula*, in *Protostars and Planets III*, ed. E. Levy, J. Lunine, & M. S. Matthews (Tucson: Univ. Arizona Press), 1031
- Yamamoto, H., & Scarlett, B. 1986, *Part. Charact.*, 3, 117